Modeling of Quantum Cascade Laser Sources with Giant Optical Nonlinearities

Christian Jirauschek
Institute for Nanoelectronics
TU München, Germany

Overview

- Modeling of quantum cascade lasers
- Inclusion of optical cavity field
- THz difference frequency generation in QCL structures
- Mode-locked QCLs and frequency combs
- Conclusion

Quantum Cascade Laser

Conventional lasers / light sources

Use optical transitions in atoms, molecules, lattices,…

- ➢ Usually in infrared, visible or ultraviolet regime
- ⇒ **Scientifically underdeveloped terahertz gap**
- ⇒ **No practical compact diode lasers in mid-infrared**

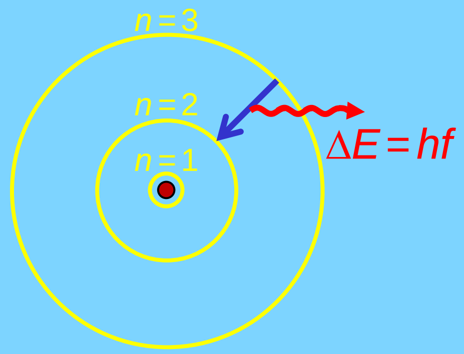

Quantum cascade laser (QCL)

Use nanostructure as “artificial atom”

- ➢ Wavelength does not depend on material, but can be tailored by “quantum engineering”
- ⇒ **QCL covers terahertz and mid-infrared**

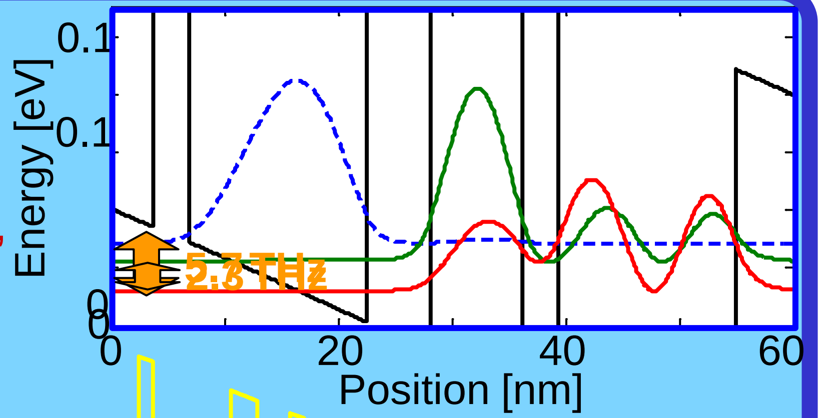

Use many transitions in a series (“cascade”)

- ➢ A single electron can emit multiple photons
- ⇒ **Increased optical power and efficiency**

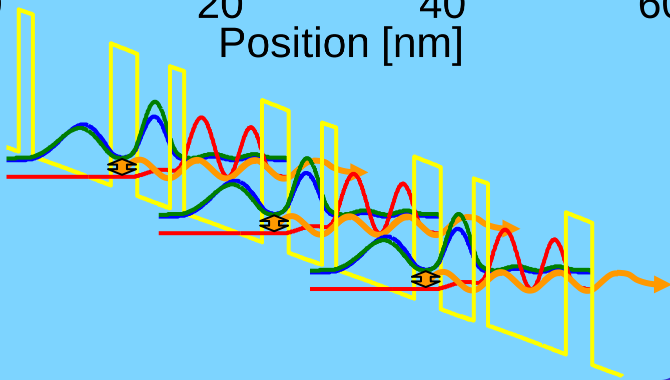

Quantum Engineering of Active Region

- Optical gain characteristics can be custom-tailored

  ⇒ Mid-infrared and THz ranges become accessible

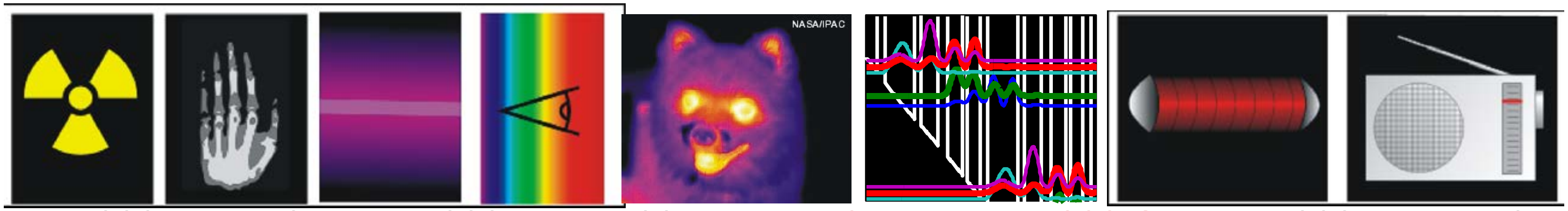

30 EHz 300 PHz 3 PHz 800 THz 400 THz 10 THz 300 GHz 300 MHz 3 Hz

Mid-infrared (>3 µm):
No practical compact diode lasers

"Terahertz gap":
Almost no practical light sources

- Artificial giant optical nonlinearities can be integrated

Frequency conversion structures

➢ **Based on frequency mixing**

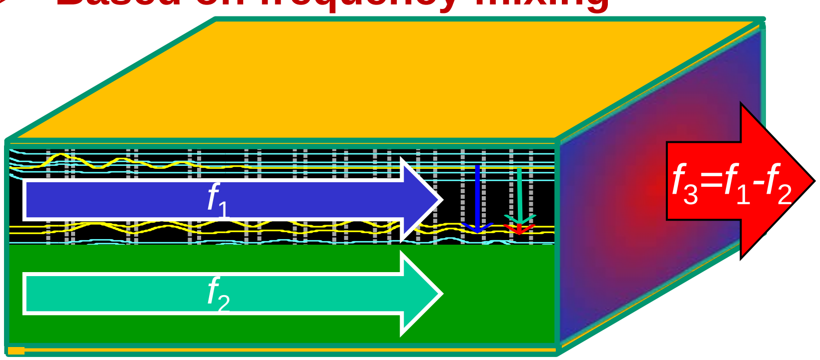

Mode-locking & frequency combs

➢ **Based on nolinear coherent interaction**

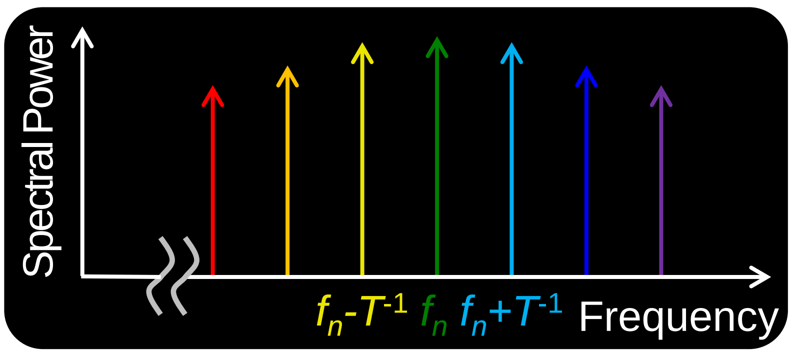

Ensemble Monte Carlo (EMC)

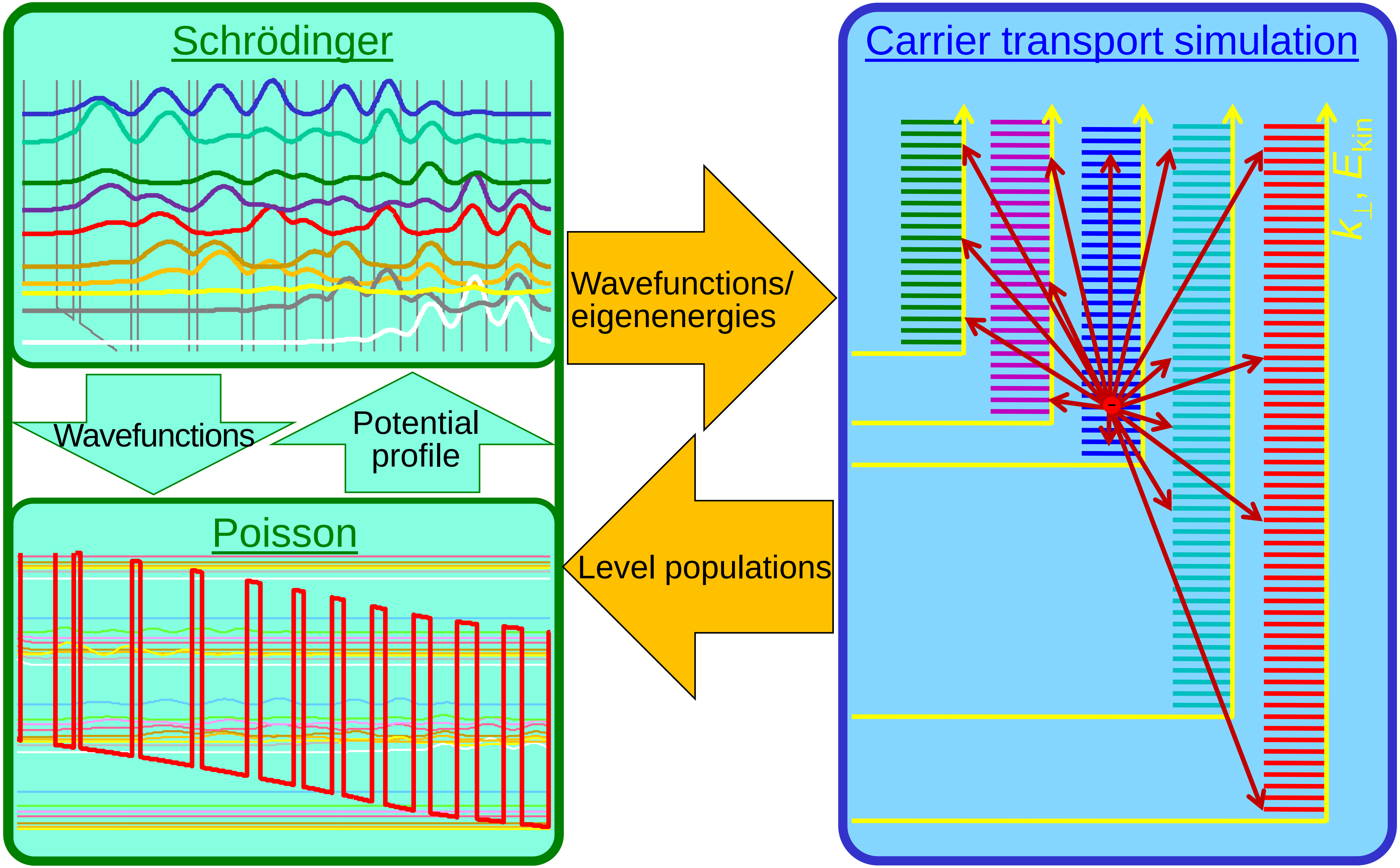

Boltzmann Equation and Scattering

Boltzmann equation for carrier distribution function $f_{n,\mathbf{k}}(t)$:

$$\frac{df_{n,\mathbf{k}}}{dt} = \sum_{s} \sum_{m,\mathbf{k}'} \left(W_{m\mathbf{k}'n\mathbf{k}} f_{m,\mathbf{k}'} - W_{n\mathbf{k}m\mathbf{k}'} f_{n,\mathbf{k}} \right)$$

$$W_{n\mathbf{k}m\mathbf{k}'}$$

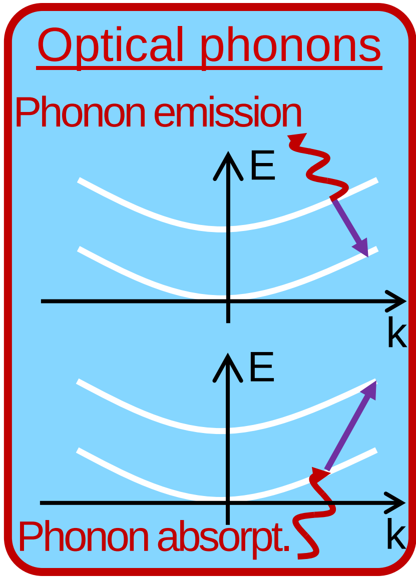

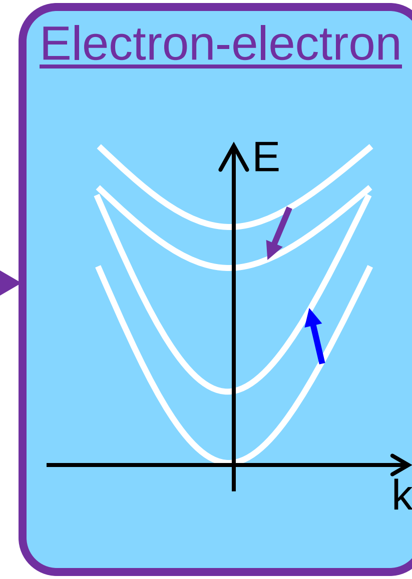

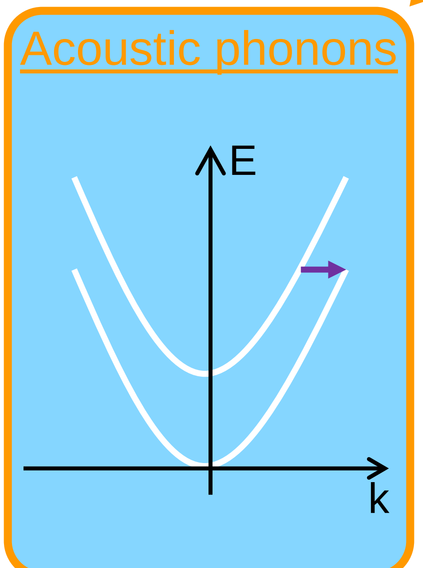

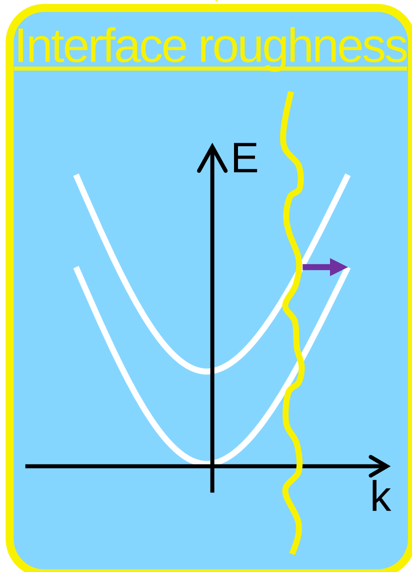

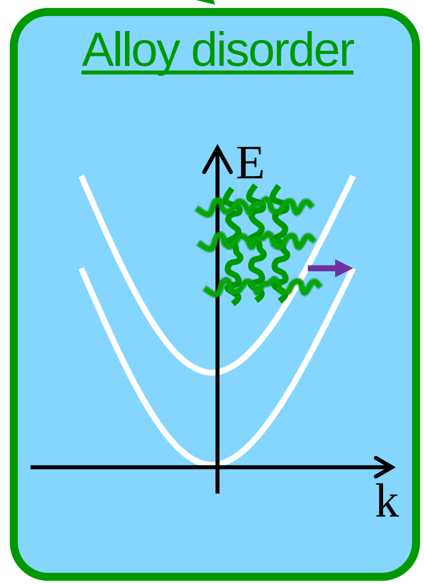

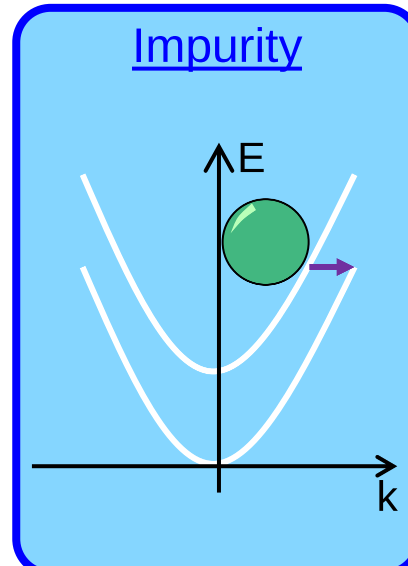

Overview

- Modeling of quantum cascade lasers
- Inclusion of optical cavity field
- THz difference frequency generation in QCL structures
- Mode-locked QCLs and frequency combs
- Conclusion

Inclusion of Optical Cavity Field

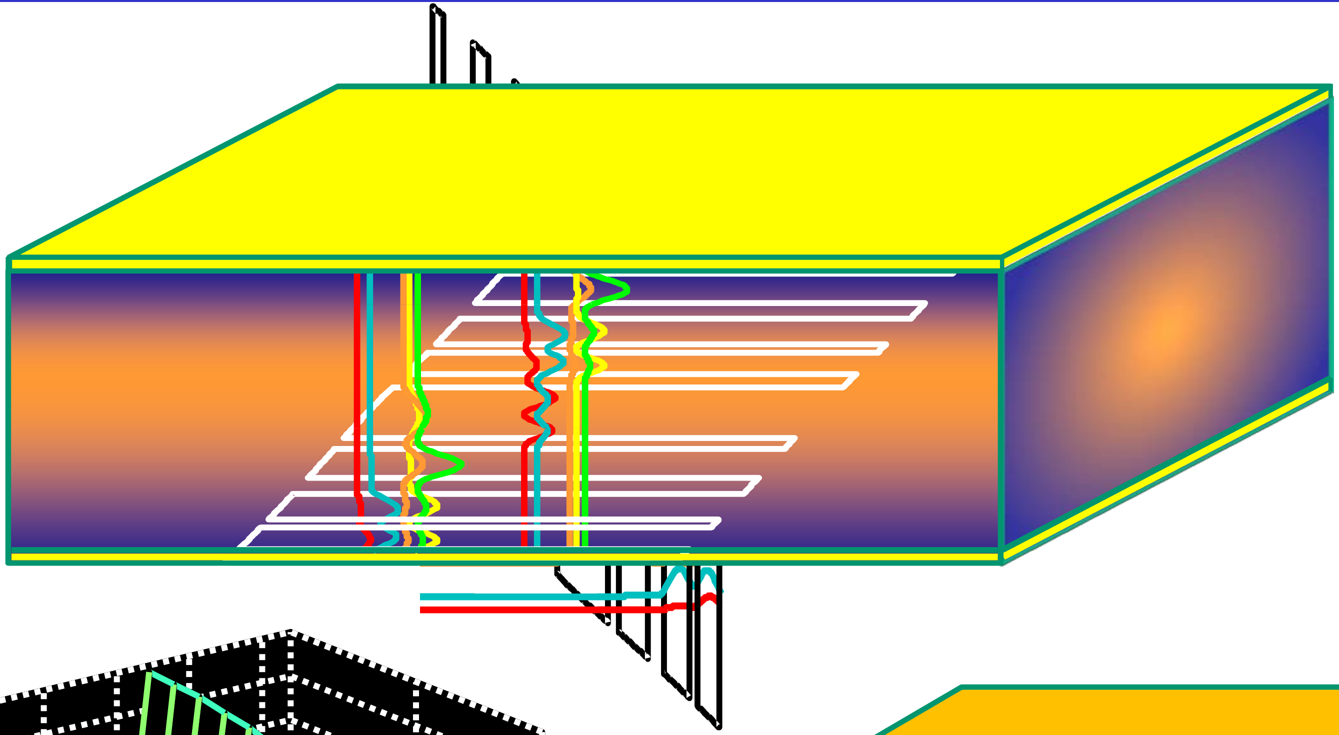

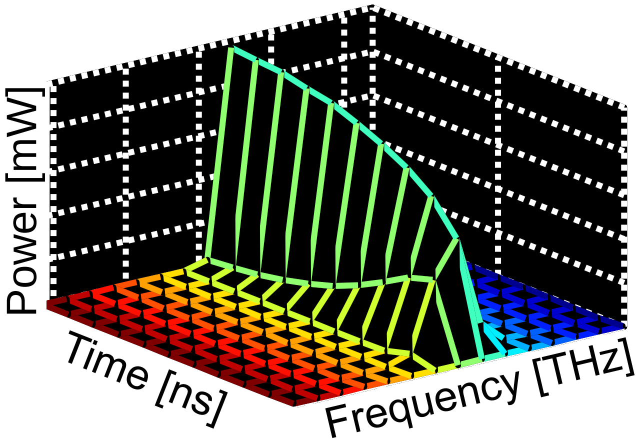

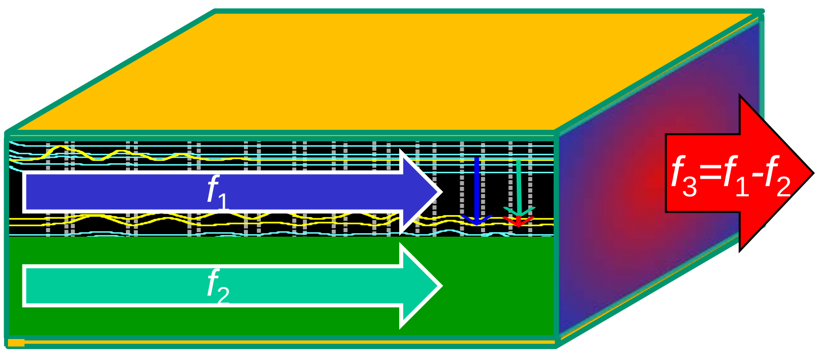

C. Jirauschek, Appl. Phys. Lett. **96**, 011103 (2010)
A. Mátyás et al., J. Appl. Phys. **110**, 013108 (2011)
C. Jirauschek, Opt. Express **18**, 25922 (2010)

C. Jirauschek et al., Opt. Express **21**, 6180 (2013)
C. Jirauschek et al., Opt. Express **23**, 1670 (2015)

Carrier-Light Coupling in Monte Carlo

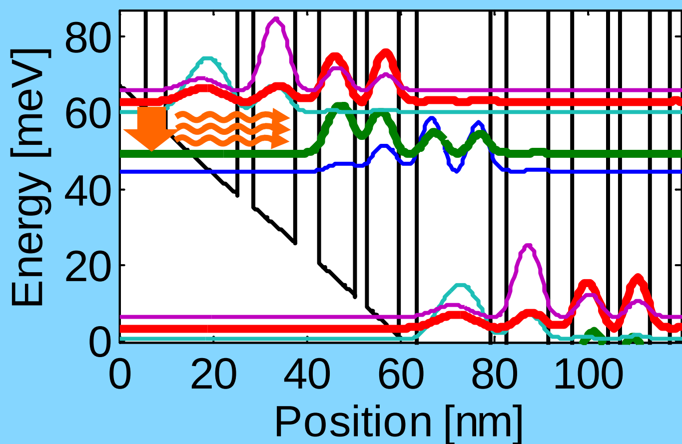

$$g(\omega) = \frac{e^2\omega}{c\varepsilon_0 n_0 \hbar L} n_E^{2D} \sum_{\substack{i,j\\ E_i > E_j}} \left| z_{ij} \right|^2$$

$$\times \int_0^\infty \mathrm{d}\varepsilon \frac{\left[f_i(\varepsilon) - f_j(\varepsilon) \right] \gamma_{ij}(\varepsilon)}{\gamma_{ij}^2(\varepsilon) + \left[\omega - \left(E_i - E_j \right)^2 / \hbar^2 \right]^2}$$

Simulation of High Efficiency Mid-Infrared QCL

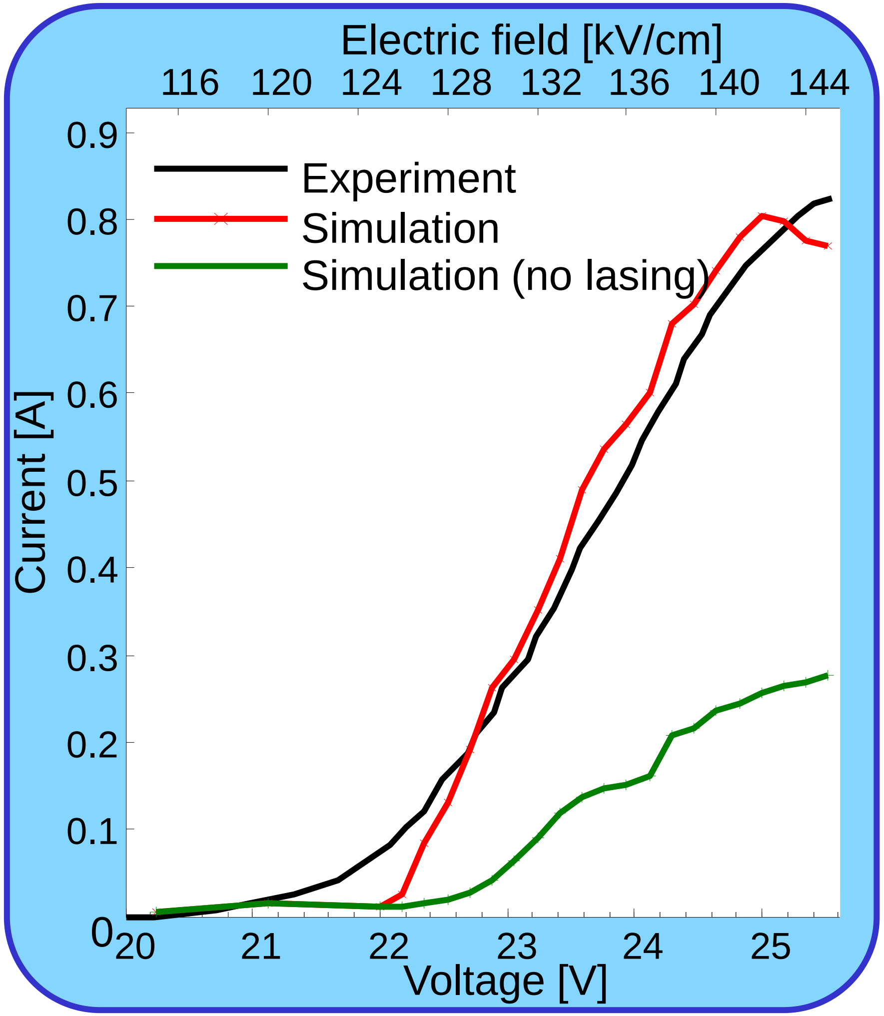

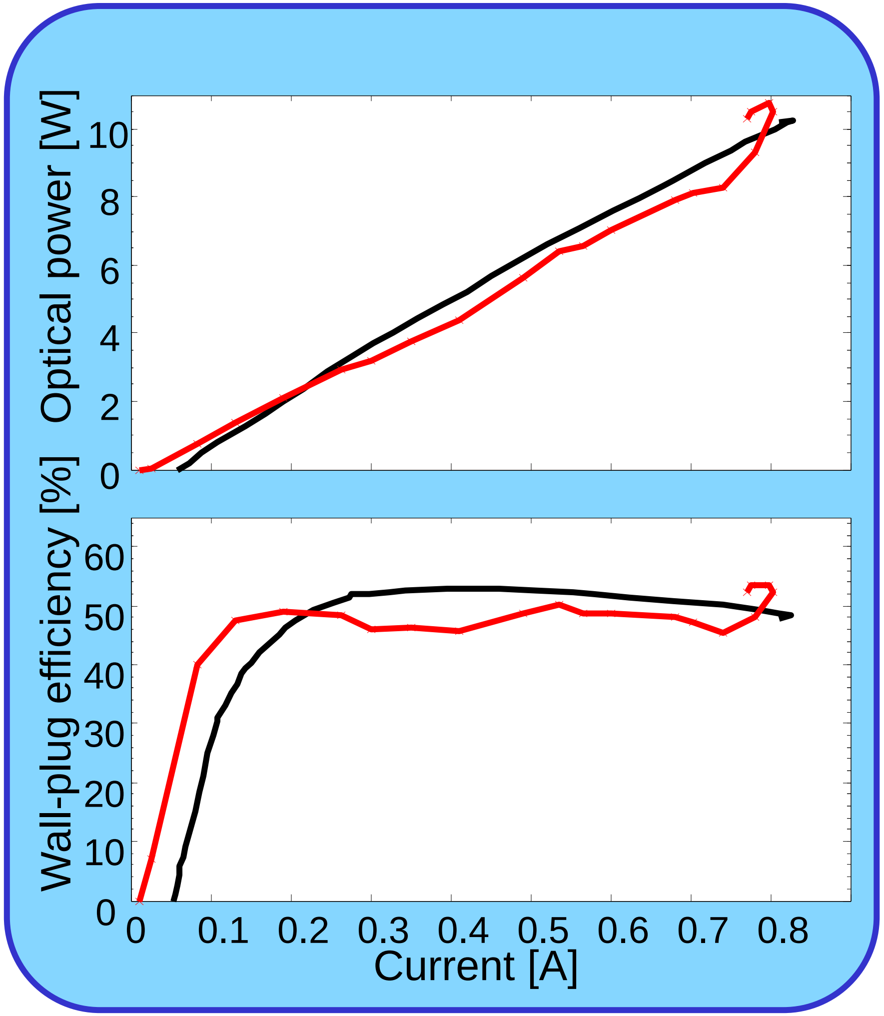

Design: Y. Bai et al., Nat. Photonics **4**, 99 (2010)

A. Matyas et al., J. Appl. Phys. **110**, 013108 (2011)

Overview

- Modeling of quantum cascade lasers
- Inclusion of optical cavity field
- THz difference frequency generation in QCL structures
- Mode-locked QCLs and frequency combs
- Conclusion

THz Difference Frequency Generation QCL Structure

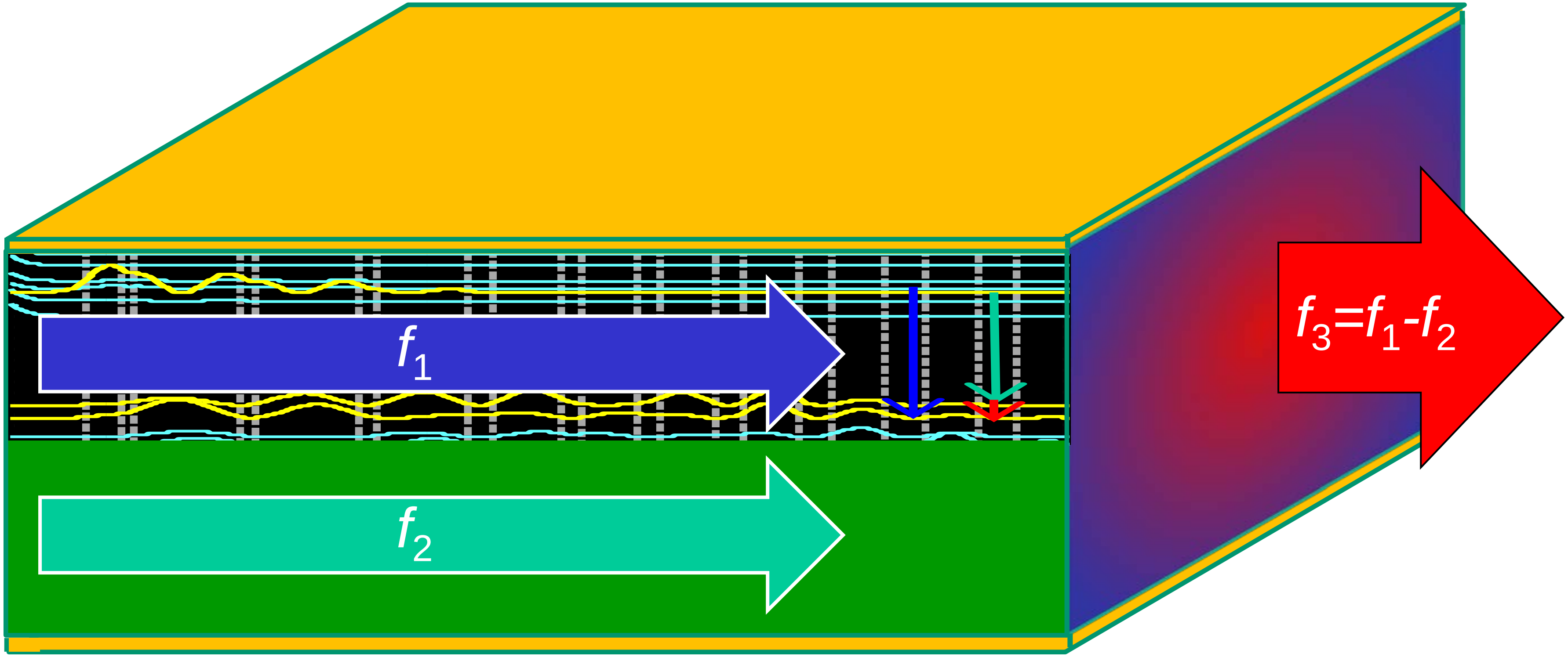

Ideal THz source

- Room temperature operation
- Broadband tunability
- THz output power in mW range

THz DFG QCL source

M. Belkin et al., Appl. Phys. Lett. **92**, 201101 (2008)

1.0-4.6 THz

Q.Y. Lu et al., Appl. Phys. Lett. **101**, 251121 (2012)

1.7-5.25 THz

K. Vijayraghava et al., Nature Comm. **4,** 2021 (2013)

1.9 mW pulsed, 3 µW cw (at room temperature)

M. Razeghi et al., Opt. Express **23**, 8462 (2015)

Modeling of Nonlinear Susceptibility

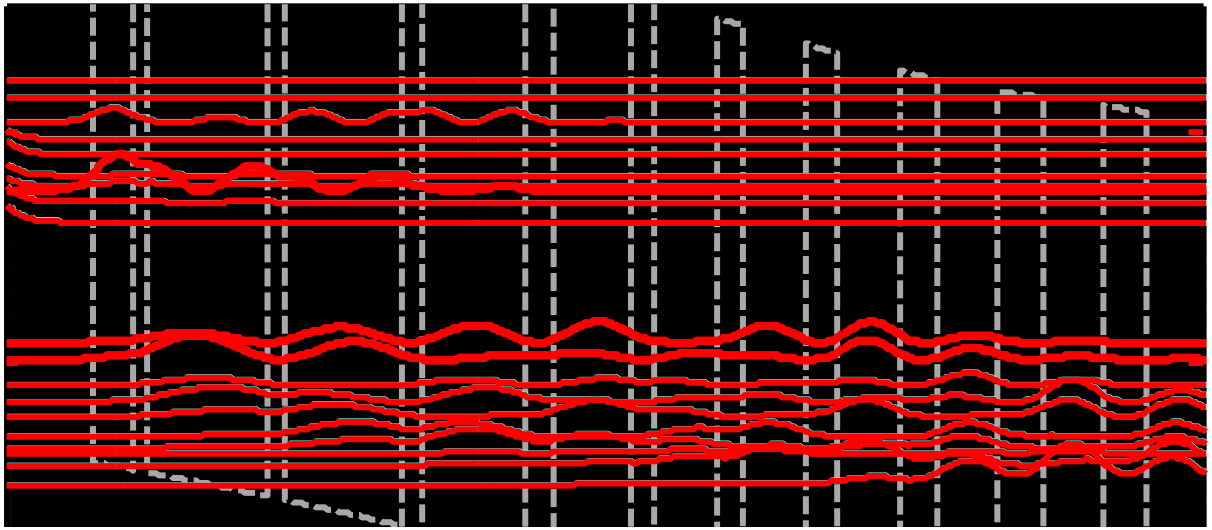

$$\chi^{(2)} = \frac{1}{\hbar^2 \varepsilon_0 L_\mathrm{P}} \sum_{\ell,m,n} d_{\ell m} d_{mn} d_{n\ell} n_E^{2D} \int_0^\infty f_\ell \left(K_{\ell mn} - K_{m\ell n} \right) \mathrm{d}\varepsilon \,,$$

$$K_{\ell mn} = \left(\frac{1}{\omega_{n\ell} - \mathrm{i}\gamma_{n\ell} - \omega} + \frac{1}{\omega_{nm} + \mathrm{i}\gamma_{nm} + \omega} \right) \left(\frac{1}{\omega_{m\ell} - \mathrm{i}\gamma_{m\ell} + \omega_2} + \frac{1}{\omega_{m\ell} - \mathrm{i}\gamma_{m\ell} - \omega_1} \right)$$

L_P:	Period length	$\gamma_{mn}(\varepsilon)$:	Optical linewidth
ε:	Kinetic energy	d_{mn}:	Dipole matrix element
$f_m(\varepsilon)$:	Distribution function	ω_{mn}:	Resonance frequency
$n_E^{2D} = m^* / (\pi\hbar^2)$:	2D density of states	$\omega_{1,2}/\omega$:	Mid-IR/THz frequencies

Multi-Domain Simulation Approach

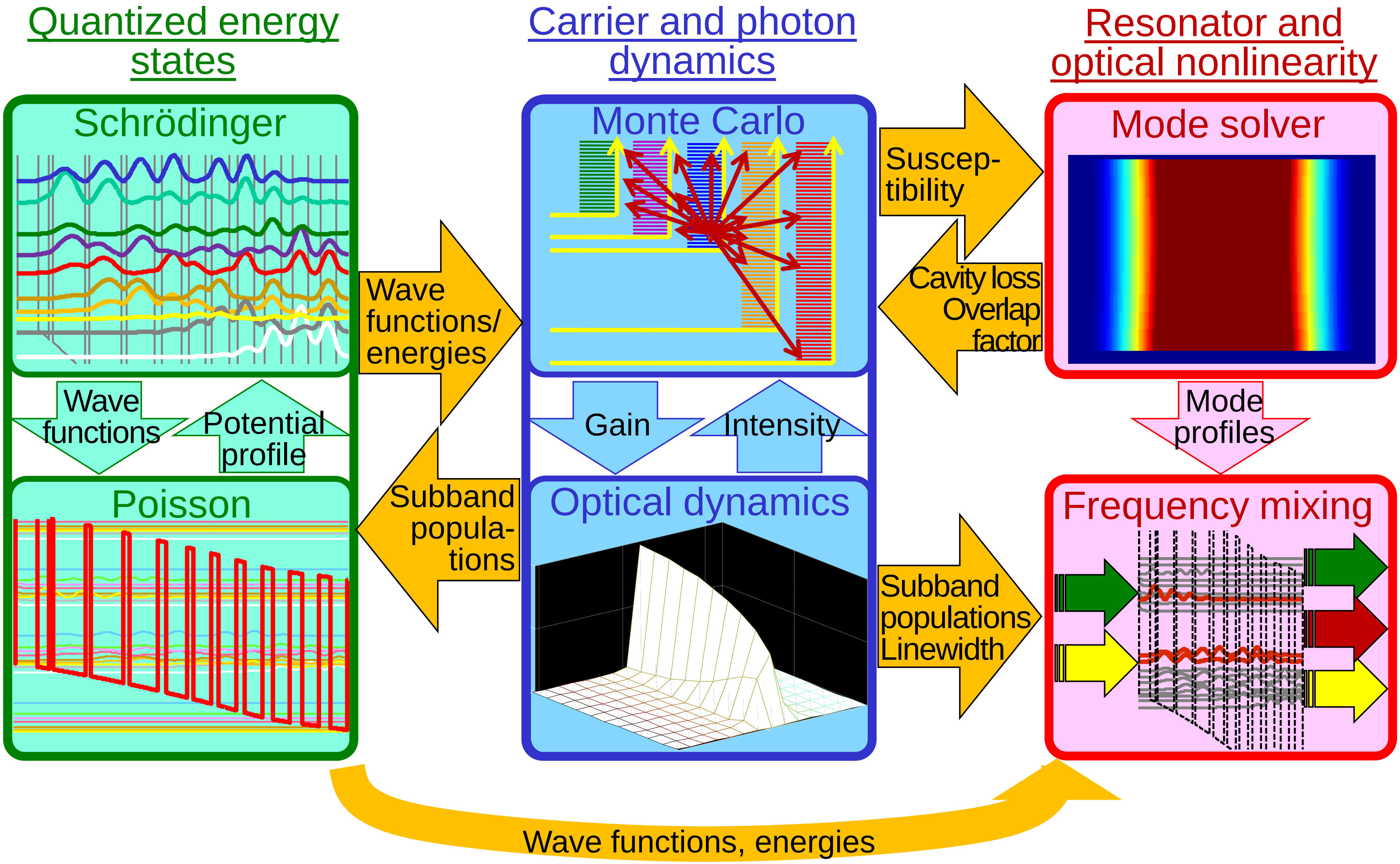

Comparison Simulation - Experiment

Mid-infrared results

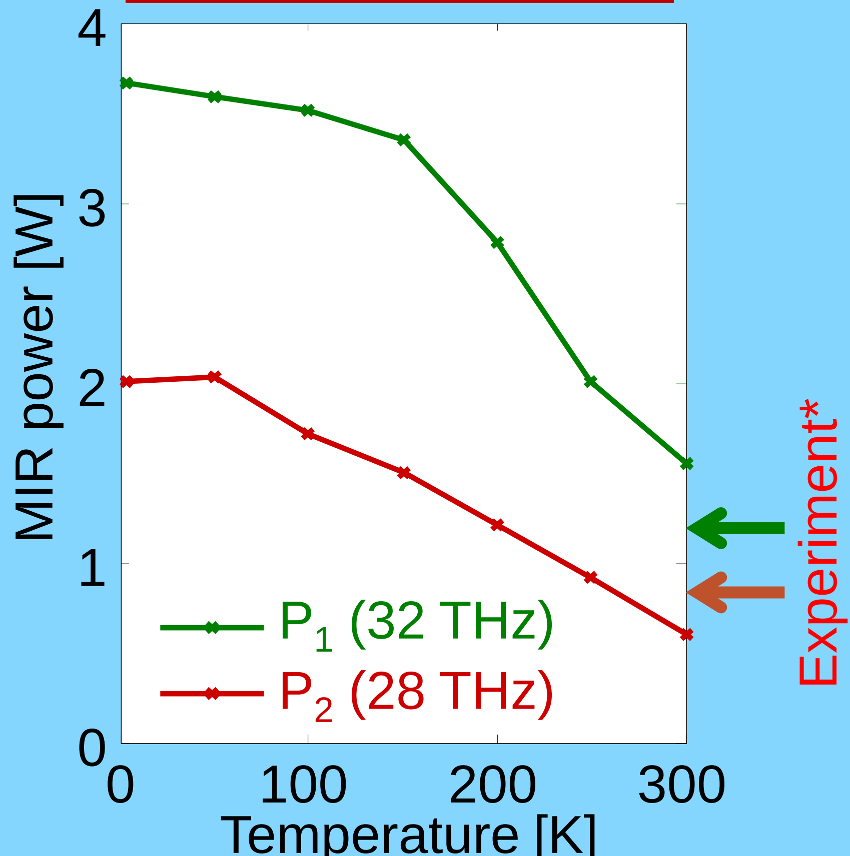

THz results

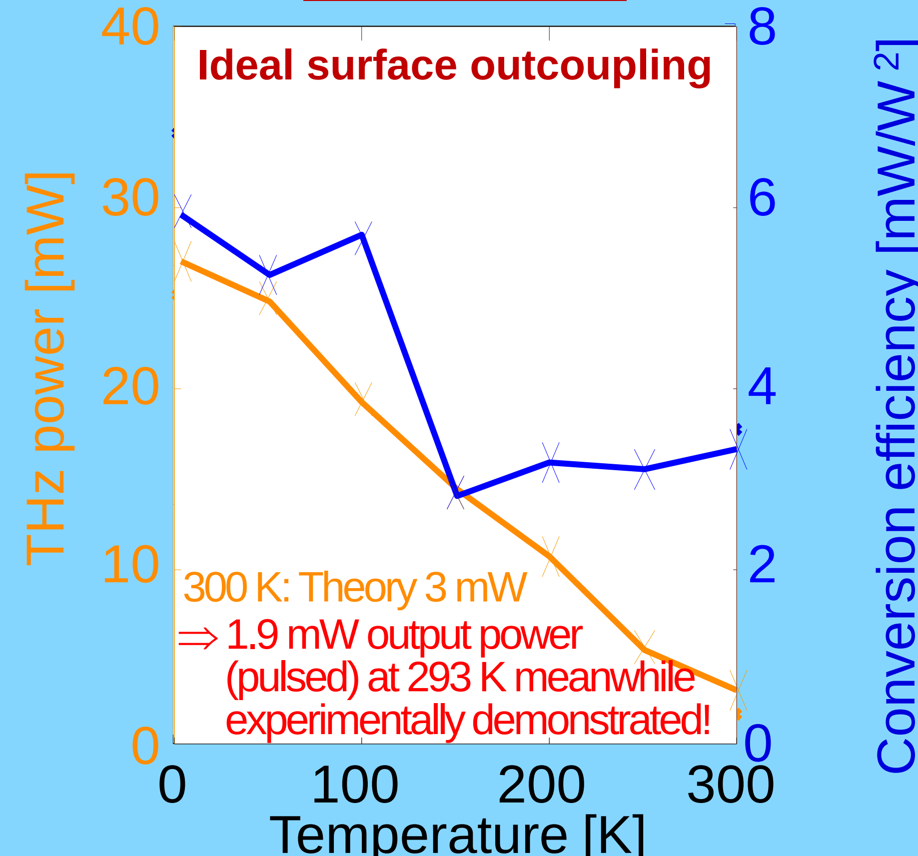

*Q. Y. Lu et al., Appl. Phys. Lett. **99**, 131106 (2011)

Extracted parameters in good agreement with experimental estimates:

- Nonlinear susceptibility $|\chi^{(2)}|$ = 44 nm/V
- THz waveguide loss *a* = 150 cm^{-1}

C. Jirauschek et al., Opt. Express **21**, 6180 (2013)

Temperature Degradation of THz Power

- Susceptibility $\chi^{(2)}$ does not degrade with temperature
- THz loss a_{THz} moderately increases with temperature
- MIR powers P_1, P_2 strongly decrease with temperature
- THz power P_{THz} strongly degrades with temperature

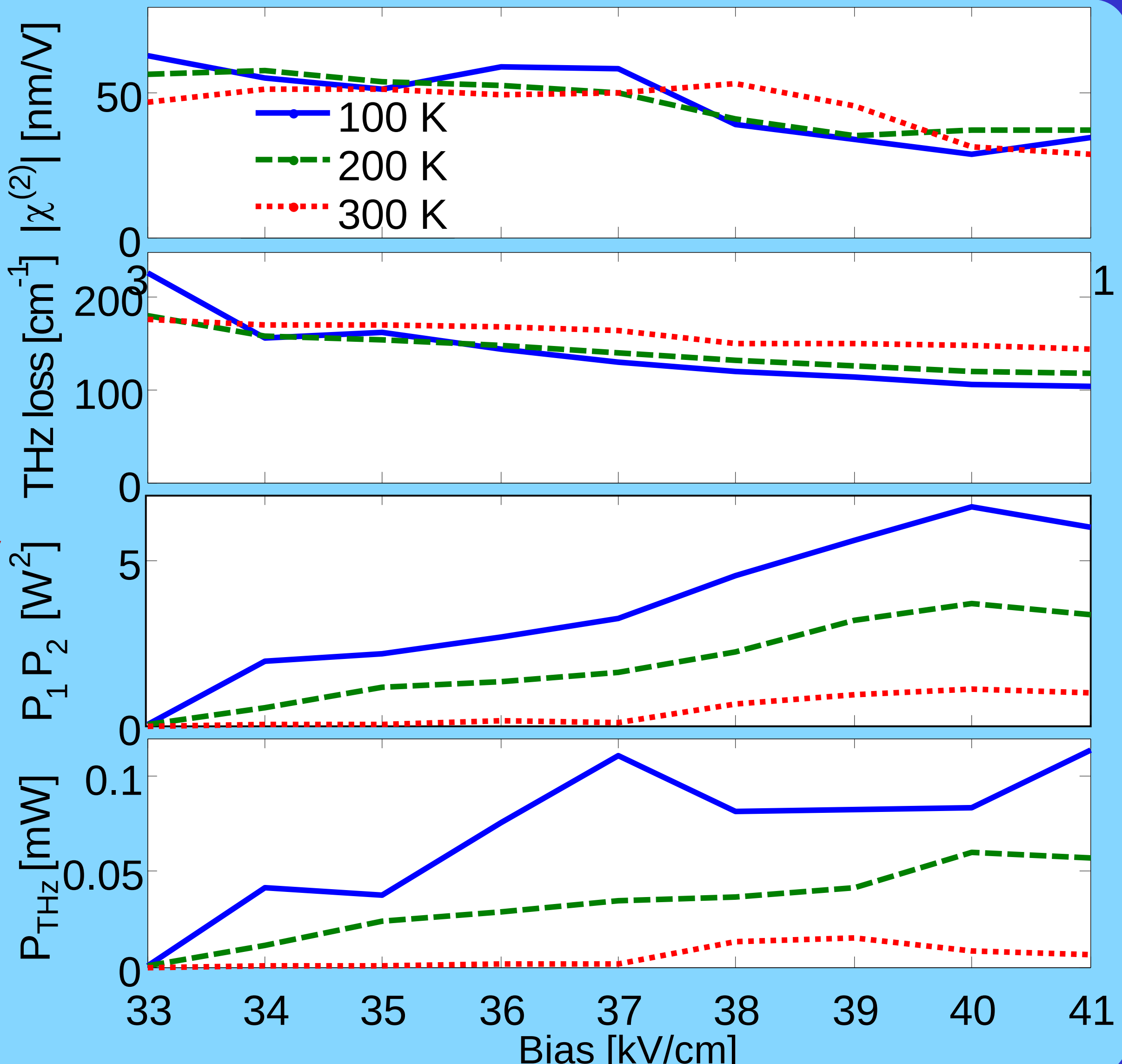

Contributions of Individual Subband Triplets

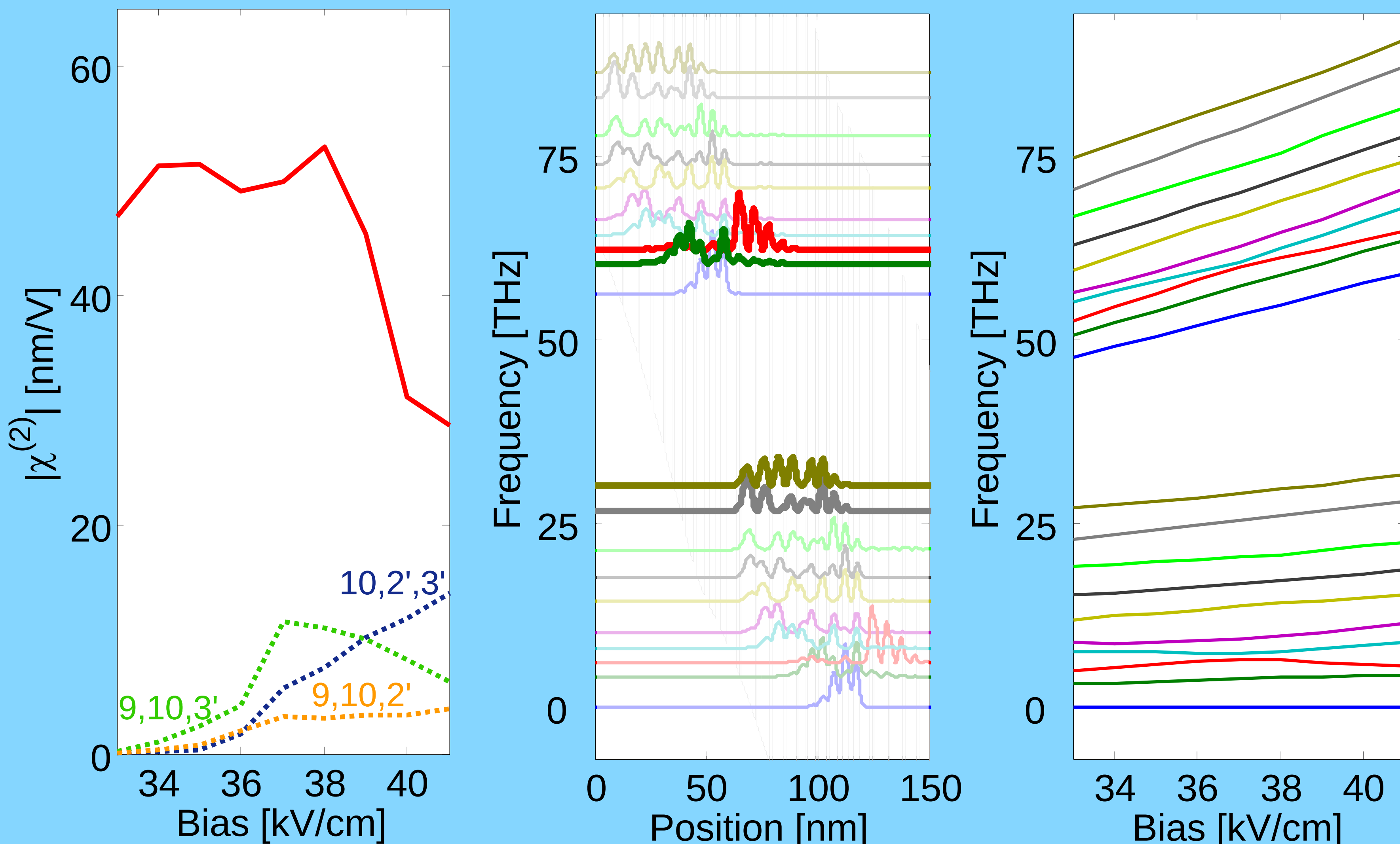

C. Jirauschek et al., Opt. Express **23**, 1670 (2015)

Susceptibility of Widely Tunable THz DFG Structure

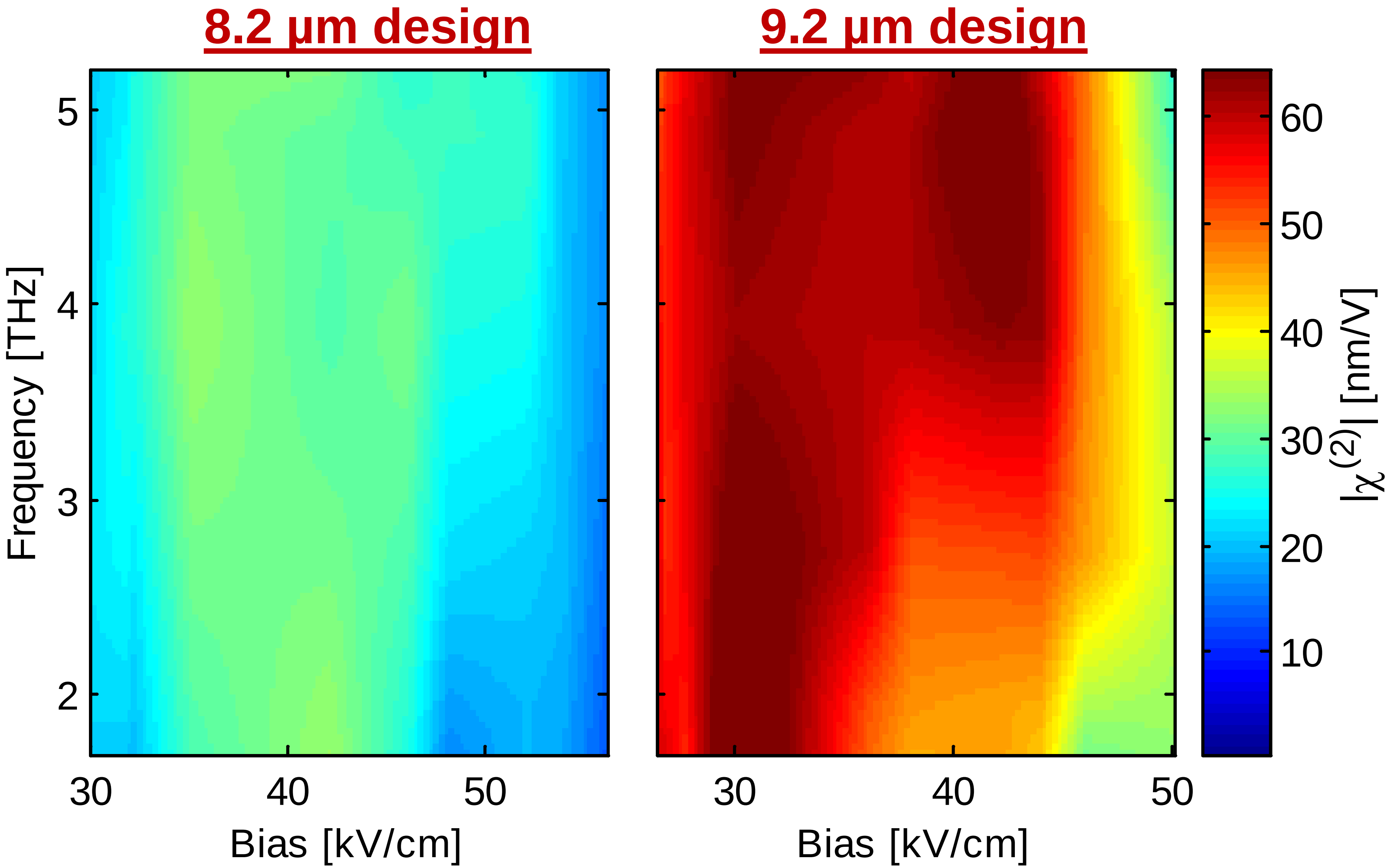

Design: K. Vijayraghava et al., Nature Comm. **4,** 2021 (2013)

Overview

- Modeling of quantum cascade lasers
- Inclusion of optical cavity field
- THz difference frequency generation in QCL structures
- Mode-locked QCLs and frequency combs
- Conclusion

Extended Maxwell-Bloch Equations

Field: $$\frac{n}{c}\partial_t E = -\partial_z E - \mathrm{i}\frac{kN\mu\Gamma}{2\epsilon_0 n^2}\eta - \frac{1}{2}\ell\left(E\right)E$$

Polarization: $$\partial_t \eta = \frac{\mathrm{i}\mu}{2\hbar}E\Delta - \frac{\eta}{T_2}$$

Inversion: $$\partial_t \Delta = \frac{\Delta_p - \Delta}{T_1} + \frac{\mathrm{i}\mu}{\hbar}\left(E^*\eta - c.c.\right)$$

Rate Equations

Field: $\frac{n}{c}\partial_t E = -\partial_z E - \mathrm{i}\frac{kN\mu\Gamma}{2\epsilon_0 n^2}\eta - \frac{1}{2}\ell(E)E$

Polarization: $\partial_t \eta = \frac{\mathrm{i}\mu}{2\hbar}E\Delta - \frac{\eta}{T_2}$

Inversion: $\partial_t \Delta = \frac{\Delta_p - \Delta}{T_1} + \frac{\mathrm{i}\mu}{\hbar}(E^*\eta - c.c.)$

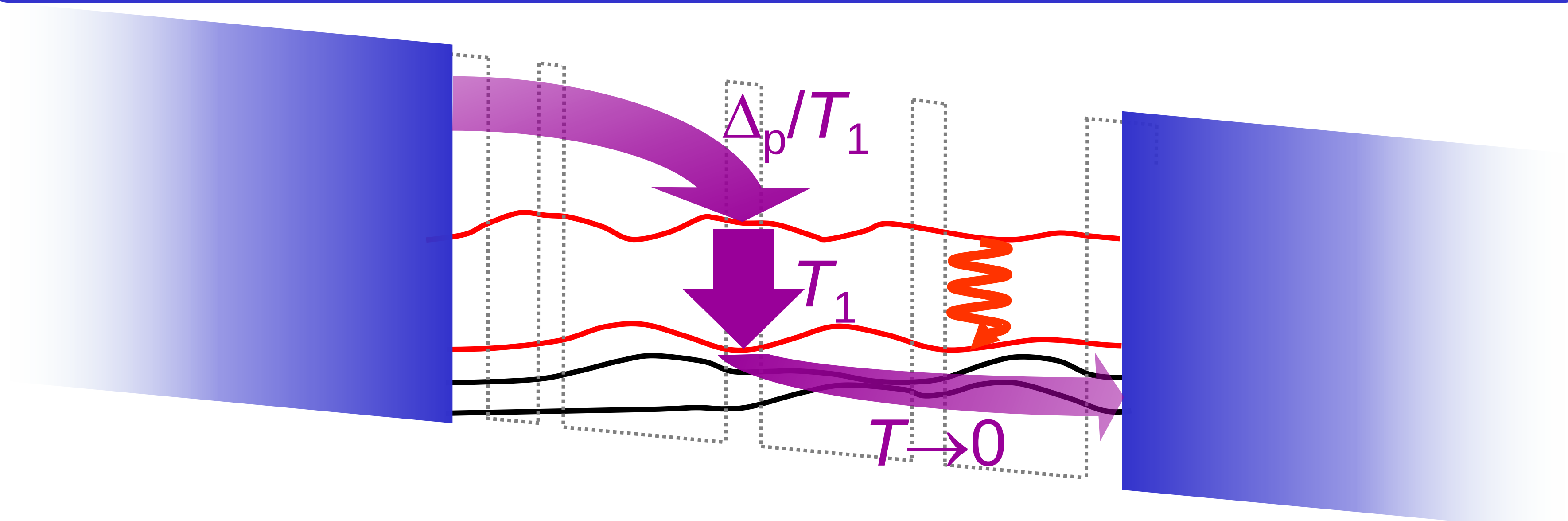

Coherent Effects

Field: $$\frac{n}{c}\partial_t E = -\partial_z E - \mathrm{i}\frac{kN\mu\Gamma}{2\epsilon_0 n^2}\eta - \frac{1}{2}\ell(E)\,E$$

Polarization: $$\partial_t \eta = \frac{\mathrm{i}\mu}{2\hbar}E\Delta - \frac{\eta}{T_2}$$

Inversion: $$\partial_t \Delta = \frac{\Delta_p - \Delta}{T_1} + \frac{\mathrm{i}\mu}{\hbar}\left(E^*\eta - c.c.\right)$$

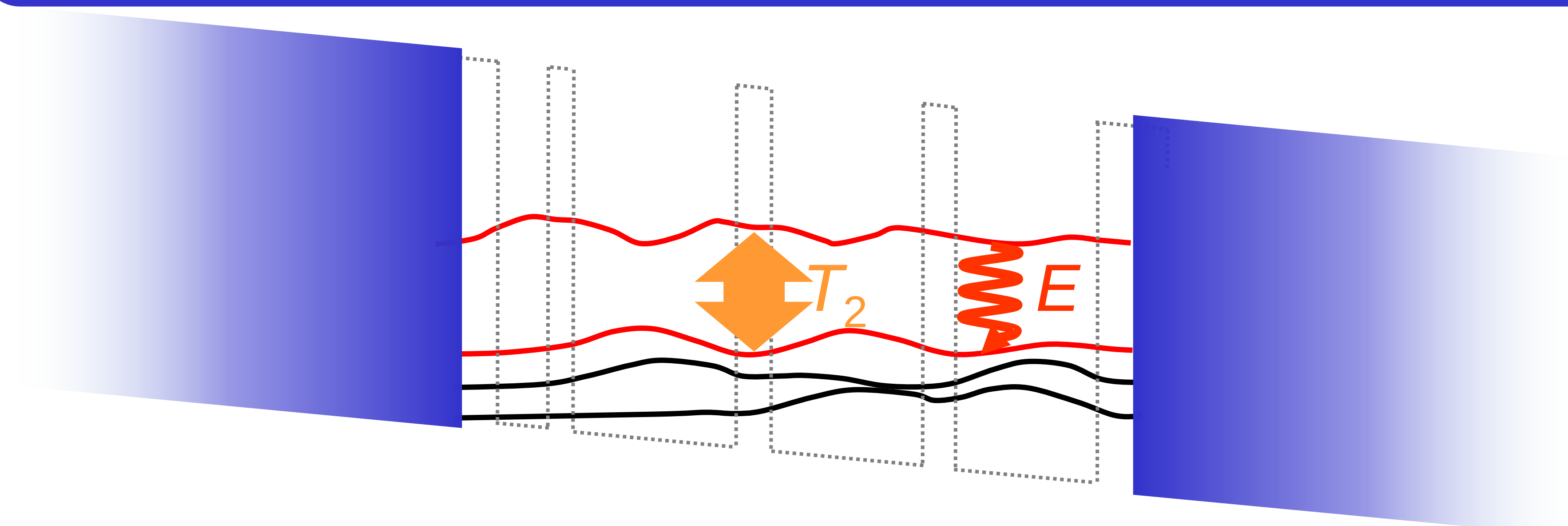

Manifestation of Coherent Effects

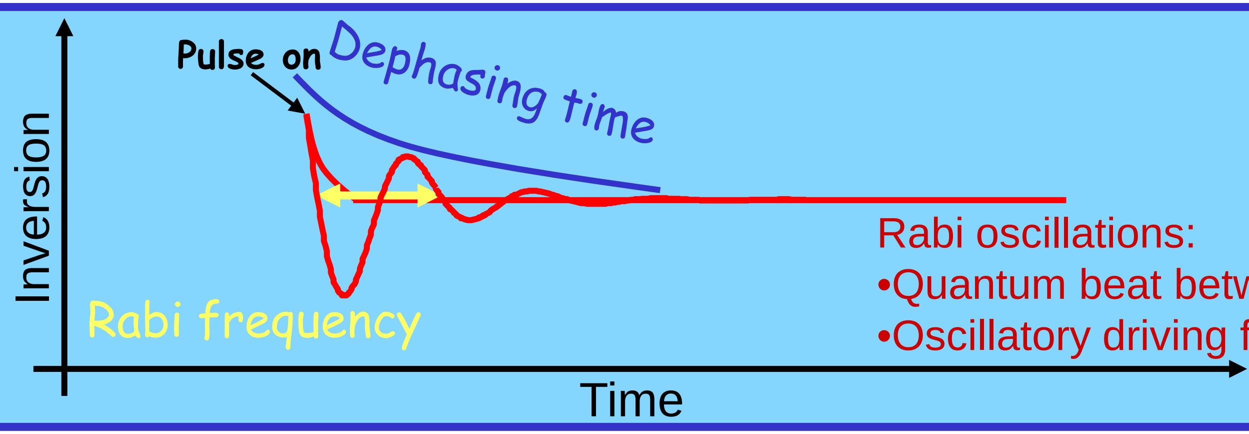

Rabi oscillations:
- Quantum beat between two states
- Oscillatory driving field

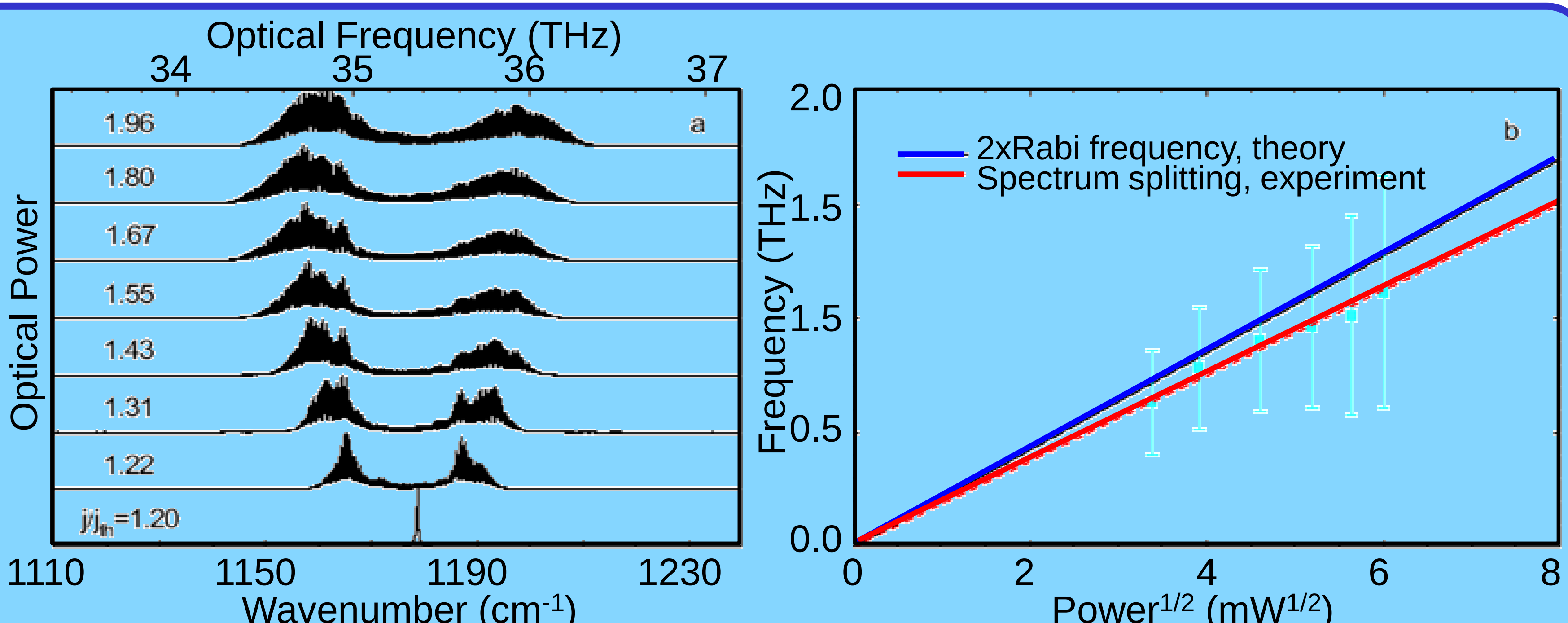

C. Y. Wang et al., Phys. Rev. A **75**, 031802(R) (2007)

Simulation of Actively Mode-Locked QCLs

Simulation

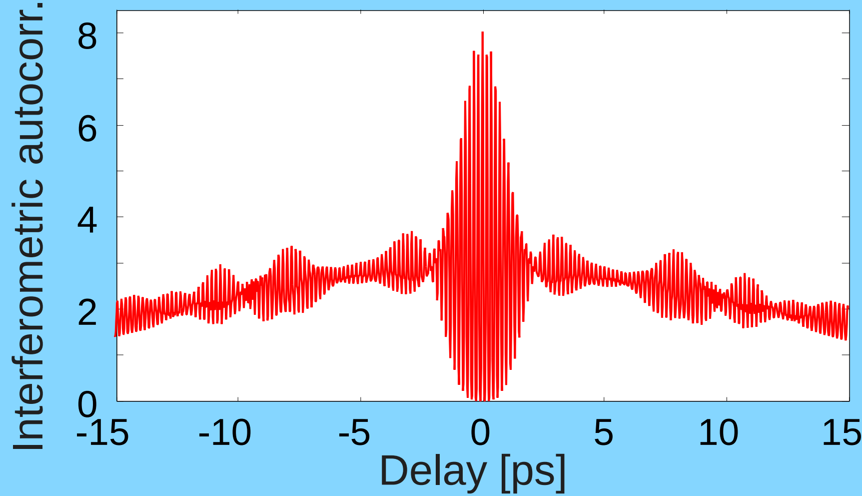

Experiment

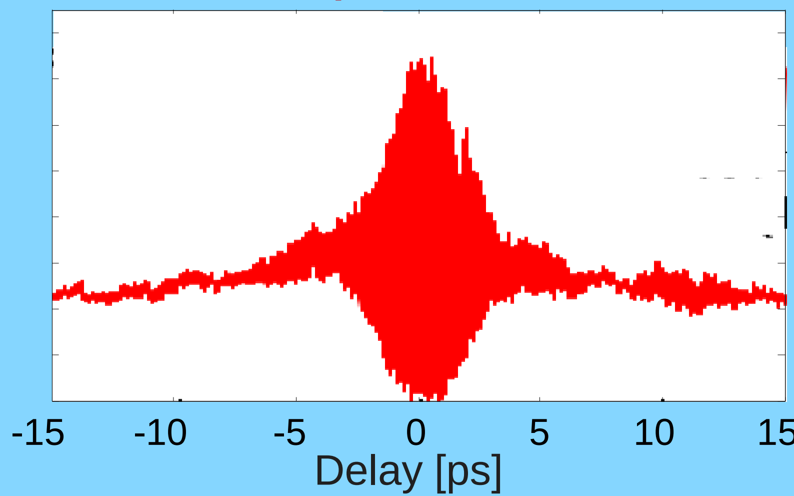

Simulated Pulse Train

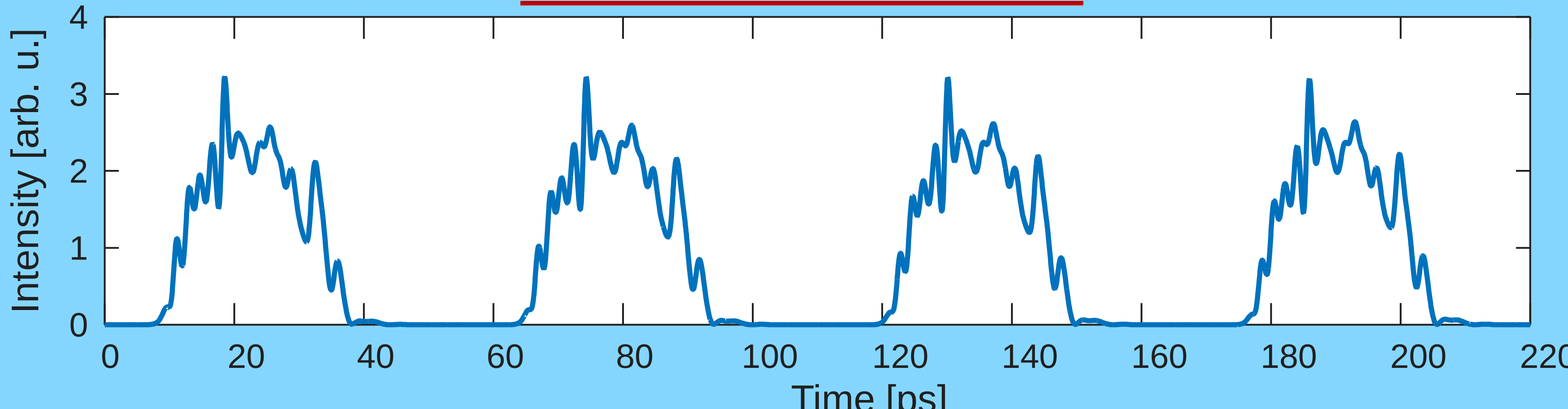

V.-M. Gkortsas et al., Opt. Express **18**, 13616 (2010)

Multi-Domain Simulation Approach

Maxwell-Bloch approach requires lifetimes/ transition rates as input parameters

- Empirical or guessed values are used, affecting the quantitative accuracy

EMC self-consistently evaluates scattering based on the corresponding Hamiltonians

- Computational burden impedes inclusion of the full spatiotemporal dynamics

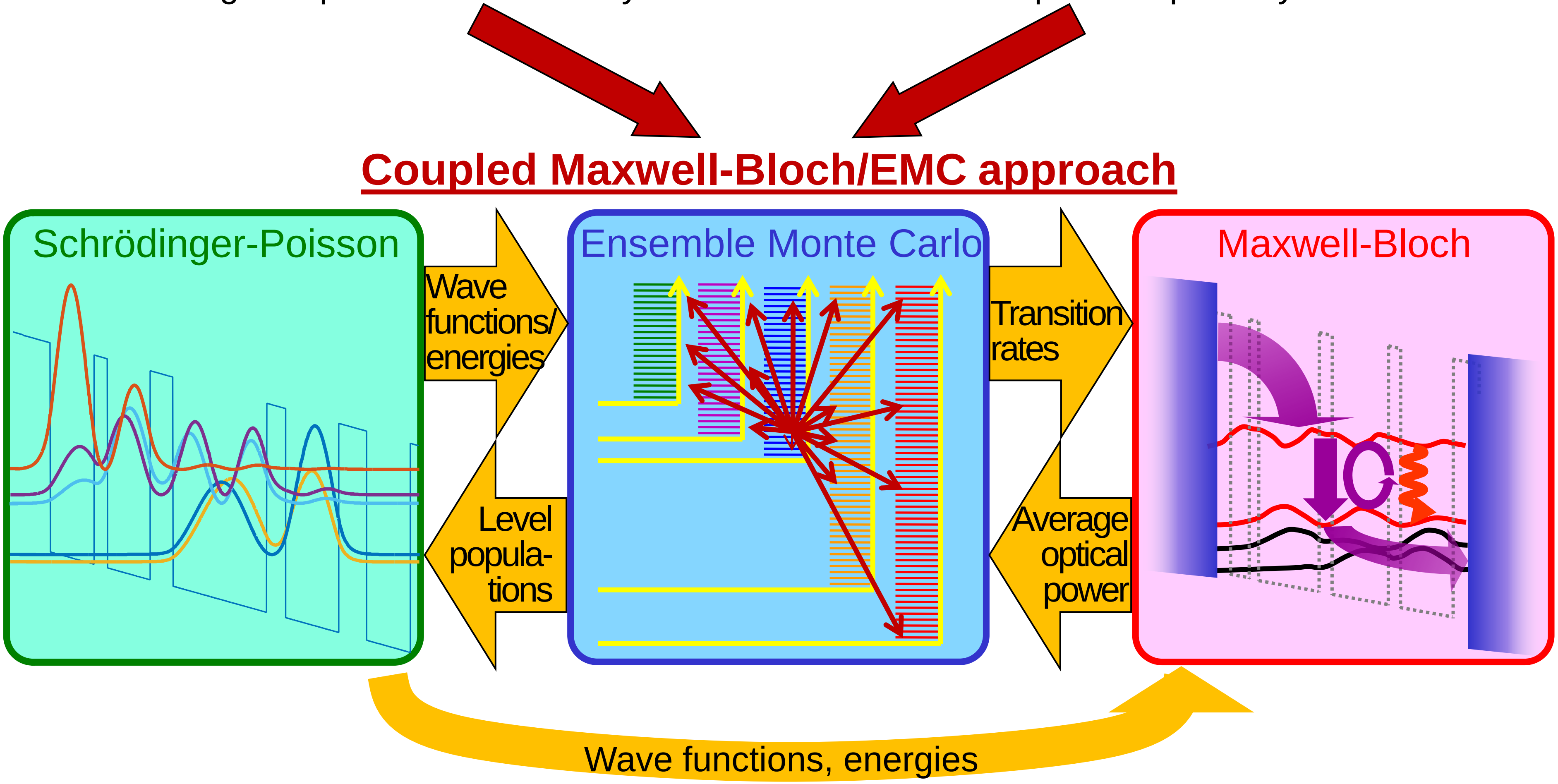

QCL-Based Frequency Combs

Periodic waveform

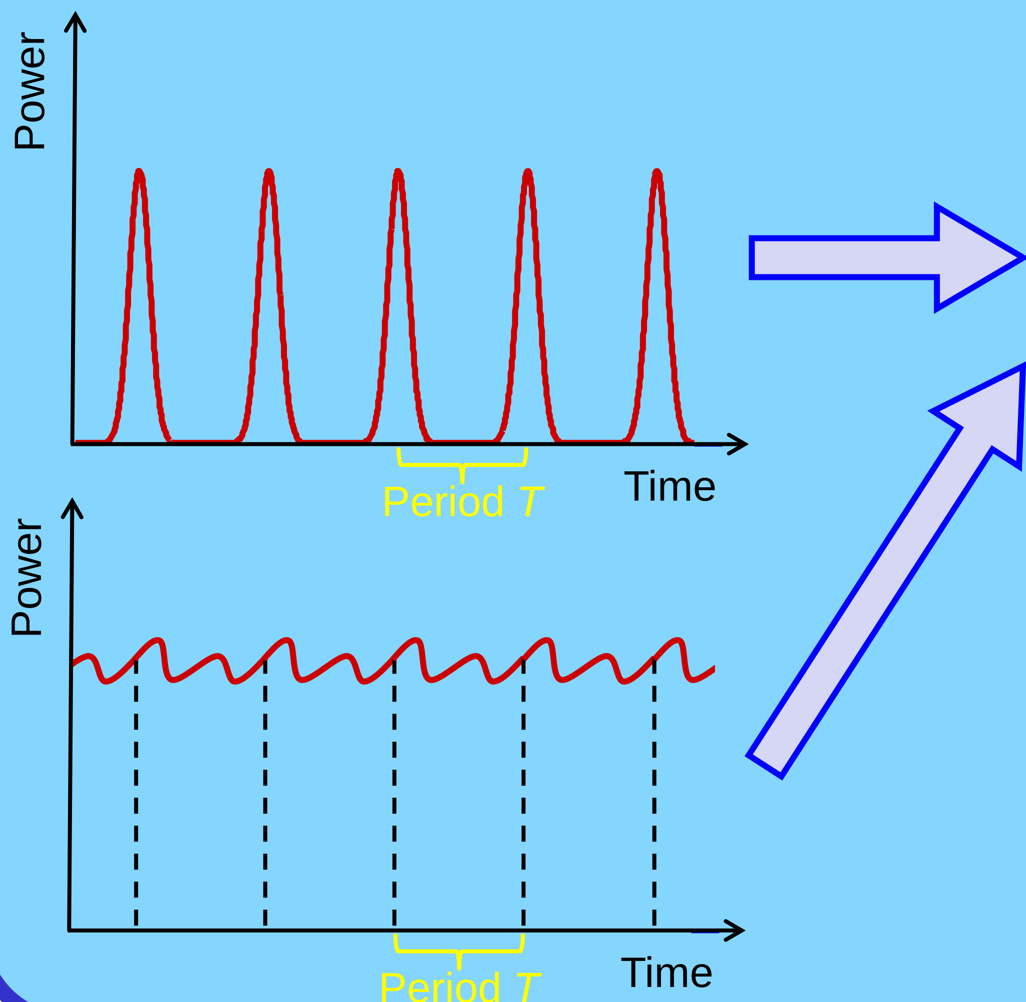

Discrete optical spectrum ≙ frequency comb

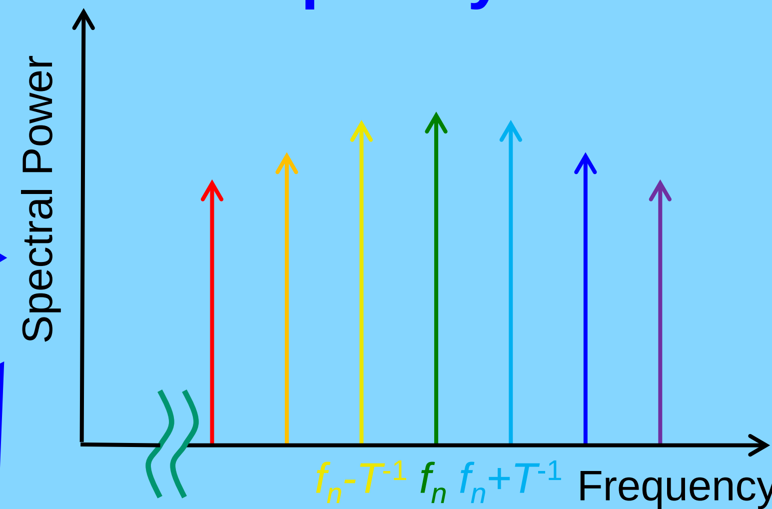

- Compact QCL-based frequency combs in mid-infrared/THz range
- Precision spectroscopy, molecular fingerprint detection (strong rotational–vibrational bands of many molecules at these frequencies)
- Modeling based on Maxwell-Bloch/ EMC approach

Terahertz Frequency Comb

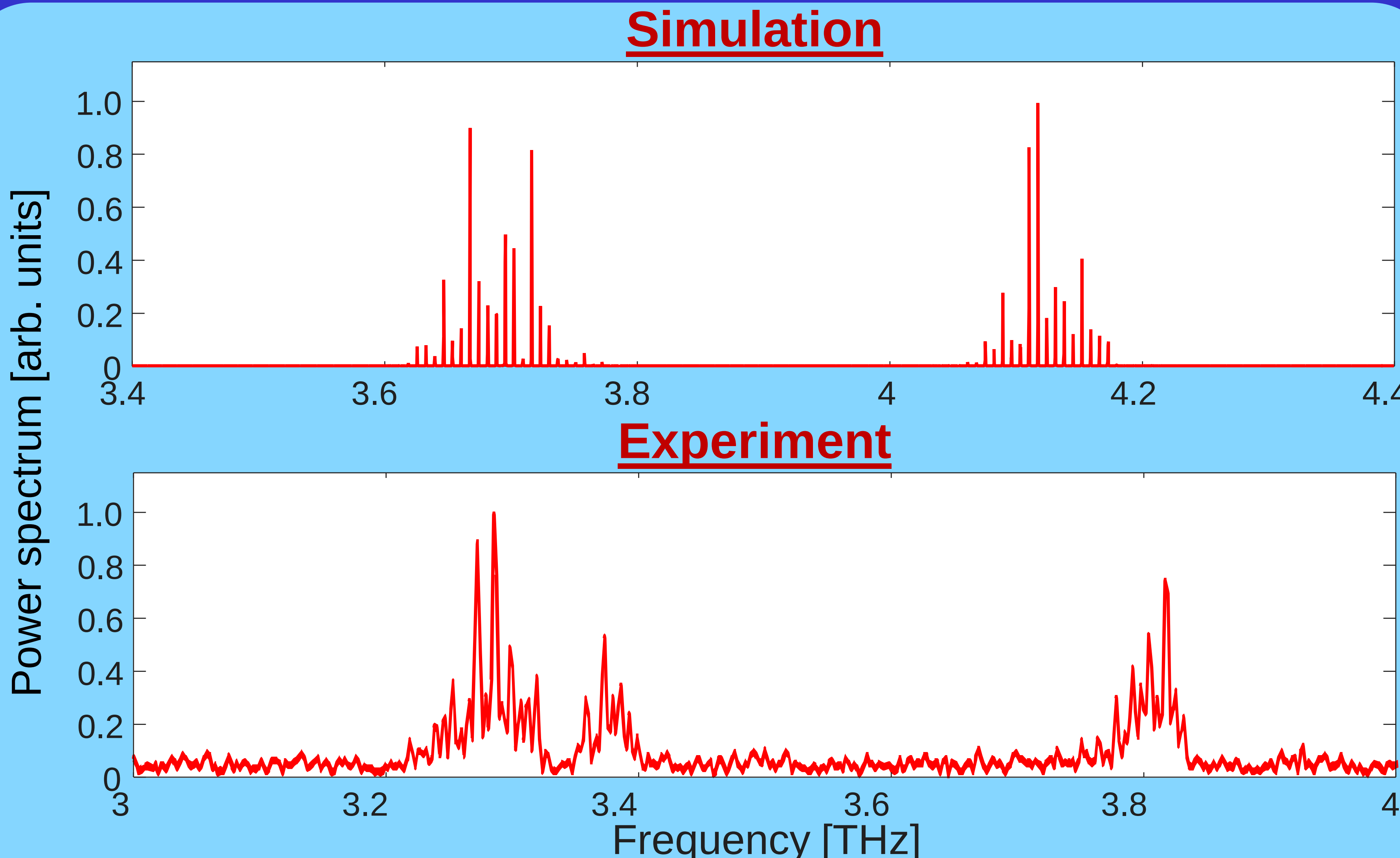

Design: D. Burghoff et al., Nature Photon. **8**, 462 (2014)

Conclusion

Ensemble Monte Carlo Method

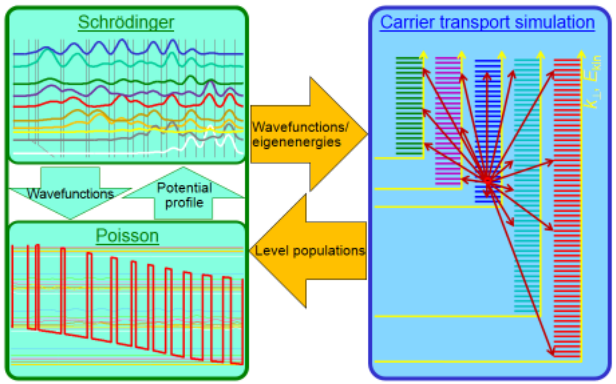

Inclusion of Optical Cavity Field

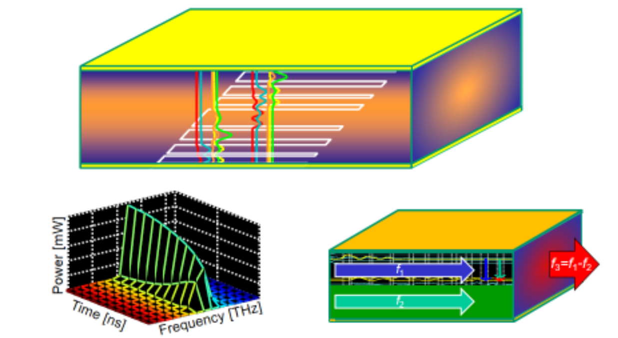

C. Jirauschek, Appl. Phys. Lett. **96**, 011103 (2010)
A. Mátyás et al., J. Appl. Phys. **110**, 013108 (2011)
C. Jirauschek, Opt. Express **18**, 25922 (2010)

C. Jirauschek et al., Opt. Express **21**, 6180 (2013)
C. Jirauschek et al., Opt. Express **23**, 1670 (2015)

THz Difference Frequency Mixing

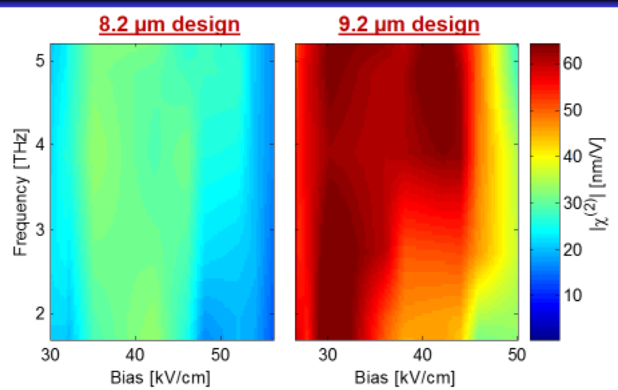

Design: K. Vijayraghava et al., Nature Comm. 4, 2021 (2013)

Maxwell-Bloch Equations

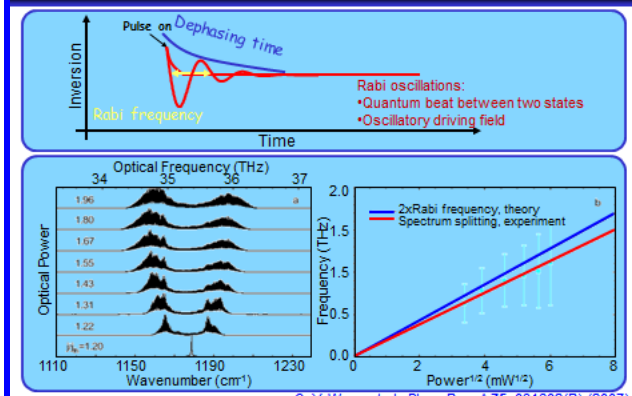

C. Y. Wang et al., Phys. Rev. A **75**, 031802(R) (2007)

C. Jirauschek and T. Kubis, Appl. Phys. Rev. **1**, 011307 (2014)

Acknowledgment

Group members

Alpar Matyas
Petar Tzenov
Hesham Okeil
Ivan Ezhov

Collaborations

Tillmann Kubis (Purdue)
Mikhail Belkin (The University of Texas at Austin)
Paolo Lugli (Technische Universität München)
Markus C. Amann (Technische Universität München)

Funding

Emmy Noether-Programm
Deutsche Forschungsgemeinschaft DFG

nim nanosystems initiative munich

Heisenberg-Programm
Deutsche Forschungsgemeinschaft